

Analysis of environmental influences in nuclear half-life measurements exhibiting time-dependent decay rates

Jere H. Jenkins^{*,a,b}, Daniel W. Mundy^c, Ephraim Fischbach^b

^a*School of Nuclear Engineering, Purdue University, West Lafayette, IN 47907, USA*

^b*Physics Department, Purdue University, West Lafayette, IN 47907, USA*

^c*Department of Radiation Oncology Physics, Mayo Clinic, Rochester, MN 55905, USA*

Abstract

In a recent series of papers evidence has been presented for correlations between solar activity and nuclear decay rates. This includes an apparent correlation between Earth-Sun distance and data taken at Brookhaven National Laboratory (BNL), and at the Physikalisch-Technische Bundesanstalt (PTB). Although these correlations could arise from a direct interaction between the decaying nuclei and some particles or fields emanating from the Sun, they could also represent an “environmental” effect arising from a seasonal variation of the sensitivities of the BNL and PTB detectors due to changes in temperature, relative humidity, background radiation, etc. In this paper, we present a detailed analysis of the responses of the detectors actually used in the BNL and PTB experiments, and show that sensitivities to seasonal variations in the respective detectors are likely too small to produce the observed fluctuations.

Key words: Ionization Chambers, Proportional Counters, Beta Decay, Gamma Decay, Energy Loss

PACS: 23.40.-s, 29.40.Cs, 23.40.-s, 29.40.-n

1. Introduction

In a recent series of papers [1, 2, 3] evidence has been presented suggesting a correlation between nuclear decay rates and solar activity. This evidence came from analyses of data from three independent sources. The first was data taken at Purdue University during a period which included the solar flare of 2006 December 13, which exhibited a statistically significant dip in the counting rate of ^{54}Mn coincident in time with the solar flare [1]. The second was data from a measurement of the half-life ($T_{1/2}$) of ^{32}Si at Brookhaven National Laboratory (BNL) [4], and the third data set was an extended study of detector stability via measurements of the decay rates of ^{152}Eu , ^{154}Eu , and ^{226}Ra at the Physikalisch-Technische Bundesanstalt (PTB) in Germany [5, 6]. The BNL and PTB data revealed periodic variations in measured decay rates which approximately correlated with Earth-Sun distance. Taken together the data of Refs. [1, 2, 3, 4, 5, 6] raise the possibility that nuclear decays are being influenced by the Sun through some as yet unknown mechanism, perhaps involving solar neutrinos.

The ^{54}Mn data presented in Ref. [1] were a series of successive four-hour counts taken over the course of two months as part of a half-life measurement. The selection of a four-hour count time allowed for a time resolution capable of detecting the solar flare, which lasted approximately 43 minutes [7]. Due to the short counting period, the counts were presumably insensitive to typical seasonal environmental effects, such as temperature, pressure, background, etc.

However, the same cannot be said of the data of Refs. [4, 5, 6] since the annually varying decay rates reported in these references could in principle arise from a number of conventional systematic influences on the detectors employed in these experiments rather than from a modulation of the decay rates themselves. The object of the present paper is to analyze the BNL and PTB data in detail in an effort to disentangle environmental influences on the detector systems used in each experiment from a possible contribution originating from the Sun, which could affect the intrinsic decay rates. The detector system used in the ^{54}Mn data set associated with the 2006 December 13 solar flare will also be discussed.

Although there are many mechanisms through which experimental detectors can be influenced by environmental factors, a useful starting point for the present analysis is the recent paper by Semkow, et al. [8] in which the authors attempt to explain both the BNL [4, 9] and PTB [5, 6, 10] data in terms of seasonal temperature variations. In what follows we will analyze these experiments in detail and show explicitly why the mechanisms proposed by Semkow et al. to explain the BNL/PTB data are not likely to be correct. This analysis can thus serve as a template for similar analyses of other past and future experiments on half-life determinations to evaluate possible seasonal environmental influences.

2. The PTB Ionization Chamber Detector

In the course of experiments at the PTB [5] which were intended to evaluate the stability of detector systems employed in the measurement of half-lives, e.g. ^{152}Eu ($T_{1/2}=4936.6(20)\text{d}$),

*Corresponding author

Email address: jere@purdue.edu (Jere H. Jenkins)

the authors reported an oscillation in the decay rate of the long-lived standard, ^{226}Ra ($T_{1/2}=1600(7)\text{y}$) used in the measurements. These fluctuations were attributed by the authors to a “discharge effect on the charge collecting capacitor, the cables and insulator to the ionization chamber electrode caused by background radioactivity such as radon and daughters which are known to show seasonal concentration changes [5]”. It was also proposed elsewhere [8] that the variations in the measured activity of the ^{226}Ra source were caused by variations of the density of the argon working gas within the detector chamber itself, caused by seasonal changes in the ambient temperature. This and other potential systematic effects, such as changes in ambient pressure, humidity, background radiation or electronic fluctuations, are indeed possible explanations for the observed variations and should be examined. An alternative proposal to these explanations, as suggested in Ref. [2], was that the oscillations of the ^{226}Ra measurements were not caused by local perturbations to the detector system, but were due to the influence of fields or particles such as neutrinos emanating from the Sun. In what follows, we will examine possible environmental influences on the detector system, and determine which of these, if any, could be responsible for the fluctuations in the ^{226}Ra measurements.

To evaluate which environmental influences may have caused the fluctuations in the detector, it is helpful to understand how the detector utilized in the PTB experiments works. The measurements were taken with a high-pressure $4\pi\gamma$ ionization chamber, Model IG12, manufactured by 20th Century (now Centronic, Ltd.), which was filled with argon to 20 atm (2 MPa) by the manufacturer, then welded shut prior to delivery to the user (Trevor Alloway, Centronic Ltd., private communication, 2009). Therefore, the number of atoms of the working gas, argon, within the detector is constant throughout the lifetime of the detector, irrespective of the external temperature, pressure or relative humidity.

The ionization chamber for the PTB experiments was operated in a “current” mode, as is typical with ionization chambers in this application. Here, the output current of the detector is generated by the collection of electron-ion pairs created by the ionization of the argon gas inside. These electron-ion pairs arise from photon interactions within the gas, and from the interaction of photoelectrons and Compton electrons generated by photon interactions in the wall of the re-entrant tube, which then enter the working gas also causing ionization. Ionization chambers operate at sufficiently high bias voltages to prevent recombination of the electron-ion pairs generated by the interactions of photons, photoelectrons, and Compton electrons in the gas. In the case of the PTB measurements, that voltage was 500V. The electrodes (anode and cathode) of the detector are contained within the chamber of the detector itself, and these collect the electrons and ions created via the radiation interactions. The current output is then the result of the of electrons collected at the anode, which is $\sim 1.44 \times 10^{-8} \text{Amp} \cdot \text{Roentgen}^{-1} \cdot \text{hr}^{-1}$ (<http://www.centronic.co.uk/ionisation.htm>, 2009). One obvious systematic variable that can be quickly examined is variation in the bias voltage. However, ionization chambers are known for their insensitivity to applied bias voltage changes,

since the ionization current is essentially independent of the applied voltage in the ion chamber region [11]. This is due to the fact that, as pointed out above, the bias voltage applied in an ionization chamber is chosen to be sufficiently high to prevent appreciable recombination of the generated electron-ion pairs, while at the same time not providing enough energy to cause multiplication of electron-ion pairs within the detector. It follows that the output current from the detector will be based solely on the number of electron-ion pairs generated by the incident radiation and collected at the electrodes within.

Since it is the ionization of the argon gas within the detector that provides the measure of the energy deposited within by the incident radiation, and thus the activity of the sources being analyzed, it follows that changes in the properties of the gas within the detector, such as the atom density, could affect the measurements. However, since the number of moles (n) of argon gas within the PTB detector is constant, the density $n/V = \rho$ of the gas will also be constant, unless the volume (V) of the detector changes. Using the ideal gas law, $PV = nRT$, where R is the gas constant, T is the temperature, and P is the pressure, it follows that if the volume is also constant (a non-constant volume will be addressed below) then the detector system is described by $P_1/T_1 = P_2/T_2$, where 1 and 2 denote the initial and final conditions, respectively. Hence, the only effect of a change in room temperature is to change the pressure inside the detector. And, since the ionization potential of argon is known to be a constant over all pressures from 1 to 200 bar [12], it follows that there should be no change in the response of the detector to changes in the room temperature if the volume of the detector is constant.

We next consider the small effects that may arise from a volume change due to expansion or contraction of the steel walls of the PTB detector as the room temperature increases or decreases. The outer case and the bulkheads of the detector chamber are manufactured using Mild Steel (Trevor Alloway, Centronic Ltd., private communication, 2009), and typical coefficients of linear expansion, α , for steel range from $\sim 9 \times 10^{-6} \text{K}^{-1}$ to $17 \times 10^{-6} \text{K}^{-1}$. For our analysis here, we will use an average value of $13 \times 10^{-6} \text{K}^{-1}$, and assume that the expansion of the metal is isotropic. Based on the stated dimensions of the detector, radius 9.25 cm and length 42.7 cm, and neglecting the small volume of the re-entrant tube (well), the initial volume, V_o , of the chamber at the initial temperature can be calculated to be $\sim 11477.9 \text{cm}^3$. The change in volume, ΔV , arising from a change, ΔT , in temperature is

$$\begin{aligned} V_o + \Delta V &= \pi [r^2 (1 + \alpha\Delta T)^2] [L(1 + \alpha\Delta T)] \\ &\cong V_o (1 + 3\alpha\Delta T), \end{aligned} \quad (1)$$

and hence the new volume of the cylinder will be 11478.3cm^3 for a 1°C increase in temperature in the room. The change in volume is thus ~ 4 parts in 100,000, and would then result in a fractional density change of -4×10^{-5} , which is two orders of magnitude smaller than the density change proposed in Ref. [8] to explain the PTB data. Additionally, it should be noted that this is a *decrease* in density, not an increase as claimed in Ref. [8], since the same number of gas atoms now occupy a negligi-

bly larger volume. We can therefore conclude that temperature increases would lead to lower density of the working medium in the detector, and thus to lower counts in the summer, as observed in the PTB data. However, in order to achieve a 1×10^{-3} fractional change in density, which would cause a corresponding fractional change in the ionization and subsequent current, the room temperature would need to change by $\sim 100^\circ\text{C}$, which is unrealistic.

In contrast to the operation of the Centronic IG12 ionization chamber employed in Ref. [5] and described above, whose density dependence is characterized $\rho(T) \approx \text{constant}$ we next consider a hypothetical detector in which the pressure, P , and the volume, V , are held constant, which is the setup studied in Ref. [8]. In this case, we find from the ideal gas law that $\rho T \approx \text{constant}$, so that $\Delta\rho = -\Delta T/T$. The change in intensity ΔI of γ -rays passing through a thickness Δx of absorbing material with density ρ is given by $\Delta I/I = \mu\rho\Delta x$ where μ is the absorption coefficient, and this leads to the familiar result [11] $I = I_o \exp(-\mu\rho x)$. Without loss of generality, we can express the counting rate (C) as $C = C_o (1 - I/I_o)$, where C_o is an appropriate normalization constant, and hence, $\Delta C/\Delta\rho = \mu x \exp(-\mu\rho x)$. To obtain the temperature dependence of C , we then replace $|\Delta\rho|$ by $|\rho|\Delta T/T$ which gives

$$\left| \frac{\Delta C}{C} \right| = \frac{\mu\rho x e^{-\mu\rho x}}{1 - e^{-\mu\rho x}} \left| \frac{\Delta T}{T} \right|. \quad (2)$$

Although this reproduces Eq. 1 of Ref. [8], we see from the preceding discussion that this result only applies to a detector for which $\rho T = \text{constant}$. This is not the case for the PTB detector, which is characterized by $\rho(T) \approx \text{constant}$ as noted above. One can illustrate the practical difference between these two cases by using the values for μ , ρ , and x quoted in Ref. [8]: $\mu = 0.07703 \text{cm}^2/\text{g}$, $\rho = 0.03567 \text{g}/\text{cm}^3$, and $x = 14.4 \text{cm}$. We find $\mu\rho x = 0.0396$, and hence, $|\Delta C/C| = 0.98 |\Delta T/T|$. By way of contrast, for the actual PTB detector, the only dependence of $\rho(T)$ on T is through the small thermal expansion of the detector chamber, as discussed above. Using a coefficient of volume expansion $\gamma = 39 \times 10^{-6} (\text{C}^\circ)^{-1}$ for steel, we find from the preceding analysis $|\Delta\rho/\rho| = 0.98 |-\Delta V/V| = 4 \times 10^{-5}$. For $T=300\text{K}$, we then find for the assumed temperature change in Ref. [8], $\Delta T = 0.91^\circ\text{C}$, $|\Delta C/C| = 3.2 \times 10^{-5}$ for the actual PTB detector. This is ~ 100 times smaller than the value $|\Delta C/C| = 2.9 \times 10^{-3}$ claimed in Ref. [8] from an inappropriate application of the ideal gas law to the actual PTB detector.

It follows from the preceding discussion that the expected effects of temperature on the IG12 ionization chamber used in the PTB measurements are much smaller than the measured fluctuations in the ^{226}Ra data. We then turn to other possible environmental effects, such as humidity, ambient air pressure, or ambient air density, which are less likely to affect the detector chamber itself since the detector is a closed system. Moreover, these effects are not likely to have an effect on the very small air gap between the source and wall of the detector well, since the $4\pi\gamma$ ionization chamber is measuring the photons (gammas and bremsstrahlung) emitted by the sources, the fluxes of which would have little dependence on the marginal air density changes in the small air gap.

We next turn to the possible contributions from background radiation of cosmic and terrestrial origins, such as the ^{222}Rn variations considered by Siegert, et al. [5], and Schrader [10] as the cause of the annual variation of the ^{226}Ra measurements. Although ^{222}Rn concentrations do exhibit seasonal as well as diurnal variations [13, 14, 15, 16, 17, 18, 19, 20], the actual activities are quite small, on the order of $15\text{-}90 \text{Bq}/\text{m}^3$, which are far below the activities of the sources being measured. Specifically, an analysis performed by Abbady, et al. in Hannover, Germany [18] (which is $\sim 60 \text{km}$ from the PTB in Braunschweig), measured indoor concentrations of ^{222}Rn inside the Centre for Radiation Protection and Radioecology (ZSR) at Hannover University. The data were collected for the period of one year, with measurements taken every two hours daily, from which monthly averages were calculated for each two hour interval. The data, shown in Table 1 of Ref. [18], do exhibit a small annual variation in the concentration of ^{222}Rn inside the ZSR offices (an institutional building which can be assumed to be somewhat similar to the institutional buildings at PTB), with the minimum and maximum concentrations occurring in February and May, respectively. Interestingly, the day/night variation shown in Ref. [18] appears to be larger than the annual variation, with the minimum and maximum occurring at 1600 and 0800, respectively. Plots of the time-averaged data and the monthly averaged data from Ref. [18] are shown in Figs. 1 and 2. The diurnal effect is clearly evident, with the early morning maximum activity concentration possibly happening while the heating, ventilation and air conditioning (HVAC) systems are off or in a lower functional state, as is typical in large institutional buildings. It should also be noted that ^{222}Rn concentrations are known to be dependent on air density, which is in turn dependent on temperature, relative humidity and pressure, as well as on precipitation. It follows that since the warmest part of the day is generally late afternoon, and the coolest is early morning, a diurnal effect is an understandable result. The annual variation is less obvious, but it appears that a maximum occurs in Summer/Autumn.

While the preceding information and analyses do not completely rule out an effect caused by ^{222}Rn , it appears that not only are the resulting activities quite small, but additionally the phase and period of the ^{222}Rn concentrations do not match those of the ^{226}Ra measurement variations reported in Ref. [5] and later analyzed in Ref. [2].

Other contributions to background in the PTB measurements would be of terrestrial and cosmic origins, such as muons, or photons from ^{40}K decay. Efforts were made by Siegert, et al. to reduce the background by use of significant lead shielding around the detector [5, 21]. However, it should be noted that the ^{226}Ra data provided by Schrader (H. Schrader, private communication, 2006) for the analysis presented in Ref. [2] were already corrected for background, which obviates the need for analyses of these background effects. Nevertheless, a discussion of those possible backgrounds is presented below. An analysis of environmental radiation at ground level was conducted by Wissmann at the PTB [19], utilizing data from the Cosmic Radiation Dosimetry Site, situated on a lake near the PTB laboratory. The results of the analysis, which corrected for fluctua-

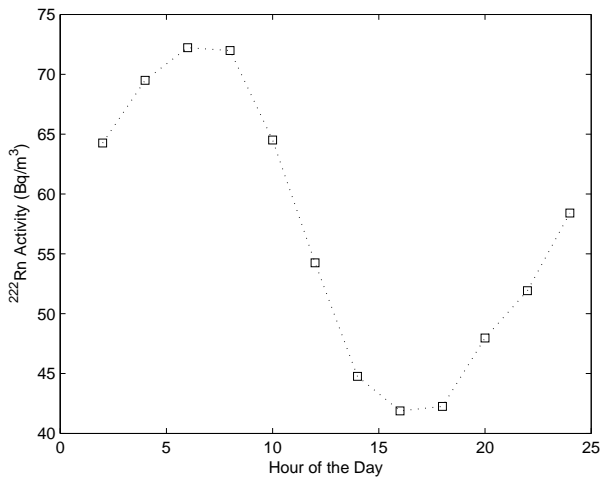


Figure 1: ^{222}Rn hourly averaged concentration obtained from Table 1 of Ab-bady et al. The data were taken at the Centre for Radiation Protection and Radioecology (ZSR) at Hannover University from July 2000 to June 2001.

tions in weather and solar effects, exhibited an annual variation of $\pm 6.9\text{nSv}\cdot\text{h}^{-1}$, which is equivalent to a dose variation equal to $\pm 1.92 \times 10^{-3}\text{nSv}\cdot\text{s}^{-1}$. Given the initial amount of ^{226}Ra in the PTB source, $300\ \mu\text{g}$, which would have had an initial activity of $11.1\ \text{MBq}$, the activity would be $\sim 88.8\ \text{MBq}$ after 40 years due to the ingrowth of the radioactive daughters. Utilizing the more conservative activity value of $11.1\ \text{MBq}$, the gamma dose rate from the source can be estimated to be $\sim 2.1 \times 10^4\text{nSv}\cdot\text{s}^{-1}$, which is 7 orders of magnitude larger than the variation in the cosmic dose rate reported in Ref. [19]. We can therefore conclude that seasonal variations in cosmic radiation background would likely have little if any effect on the PTB detector system.

Returning briefly to the background radiation from ^{222}Rn , it should also be noted since ^{226}Ra decays to ^{222}Rn , the decay chain of ^{222}Rn is identical to the decay chain of ^{226}Ra . If the ^{222}Rn daughters are in equilibrium with the relatively constant ^{222}Rn concentration of $\approx 55\ \text{Bq}$, the activity of ^{222}Rn and its daughters at any time will be $\approx 300\text{Bq}$, which equates to a gamma dose rate of $\approx 0.58\text{nSv}\cdot\text{s}^{-1}$. This value is five orders of magnitude smaller than the dose rate of the ^{226}Ra source itself. Hence, it can be safely assumed that even with a variation of the atmospheric ^{222}Rn concentration of $\pm 100\%$ (which is significantly larger than the actual variation noted in Ref. [18]), the even larger activity of $\approx 600\text{Bq}$ would yield a new gamma dose rate of $\sim 1.16\ \text{nSv}\cdot\text{s}^{-1}$, which is still four orders of magnitude smaller than the dose from the ^{226}Ra source itself. This effectively rules out a discharge effect on cables, etc. arising from charged particles or photons produced by ^{222}Rn daughters as the cause of the measured variations reported in Ref. [5].

3. The PTB Solid State Detector

The ^{154}Eu and ^{155}Eu samples studied by Siegert, et al. [5] were measured with three different semi-conductor detectors as

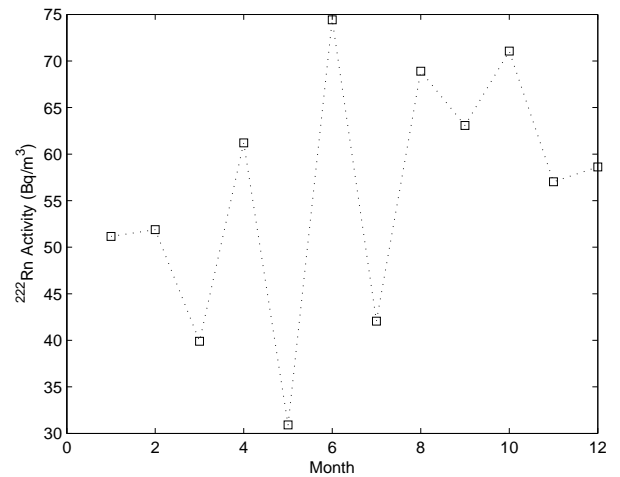


Figure 2: ^{222}Rn monthly averaged concentration obtained from Table 1 of Ab-bady et al. The data were taken from June 2000 through May 2001, and are arranged here January through December. See caption to Figure 1 for further details.

part of the evaluation of detector system stability previously discussed. In the course of these measurements, a separate ^{152}Eu calibration source was used to measure the changes in efficiency of the Ge(Li) detector which was one of the three semi-conductor detectors examined. A plot of measurements of the efficiency of a Ge(Li) detector versus time, which is presented in Fig. 2 of Ref. [5], exhibits a similar period of 1 year, shifted by half a period (or about 6 months), with an amplitude of about 0.5%. The efficiency of a detector is determined by comparison of the measured counts taken with the detector to the expected output of a known source in a fixed geometry. Thus, for the Ge(Li) measurement of the ^{152}Eu point source, the minima of the efficiency curve represent a deficit in counts (with respect to the expected counts based on the known activity and half-life of the standard), while the maxima represent an excess of counts. Specifically, the minima of the efficiency plot fall near the beginning of the calendar year for the Ge(Li) detector, which is opposite to the signal seen in the ionization chamber measurements of ^{226}Ra . This appears to call into question the conclusion of Jenkins, et al. [2] that decay rates are simply dependent on the distance of the Earth from the Sun. However, the fact that the period of the ^{152}Eu data is the same, but shifted by half a period, still suggests a possible link to the Earth-Sun distance.

This possibility is supported by an examination of the decay modes of ^{152}Eu which has two branches, K-capture (72.10%) and β^- decay (27.90%) [22]. The 1408 keV photon measured with the Ge(Li) detector [5] only arises from the K-capture branch, and is seen in 21.07% of the decays (there is no photon of that energy in the β^- decay branch)[22]. In contrast to the Ge(Li) detector, the ionization chamber is incapable of discriminating among the different photons measured, and hence could not track the 1408 keV photon separately, as it would be lost in the sum of all the photons emitted by the sample. The phase of the ^{152}Eu data could thus be understood if K-capture

modes responded to an external influence oppositely from β^- decays.

In Refs. [1, 2] the conjecture was put forward that a field or particle emanating from the Sun, possibly neutrinos, might be enhancing or interfering with the decay of radioactive nuclides. Since the quantum mechanical details of the K-capture and β^- decays are quite different, it is in fact possible that the response of the K-capture branch would be different from that of the β^- decay branch. If these were in fact opposite effects, i.e. the decay rate for the β^- decay branch would be increasing when the K-capture rate was decreasing, these competing effects would tend to damp out any fluctuations. That such a possibility could actually occur is supported by data from ^{54}Mn (which also decays via K-capture) acquired during the solar flare of 2006 December 13, [1]. It was observed that the ^{54}Mn count decreased from the expected rate during the three-day period encompassing the solar flare. Thus, if we assume that the solar neutrino flux increased during the solar flare, then the response of ^{54}Mn and ^{152}Eu to increased solar flux would have the same phase in the sense that both decay rates decreased in response to an increase in solar neutrino flux.

4. The BNL Proportional Counter

We next turn to an examination of the environmental sensitivity of the gas proportional counter and sample changing system used by Alburger, et al. [4] and Harbottle, et al. [9] to measure the half-life of ^{32}Si . The detector in question was cylindrical, ~ 1.5 in. diameter, 2 in. depth, with a 1 in. end window, operating on P-10 gas. The detector pressure was held constant by a device on the gas outlet vented to a barostated enclosure to limit fluctuations in the density of the P-10 gas. The detector itself was mounted on an automatic precision sample changer, which was entirely contained within the aforementioned barostated enclosure, as described in Refs. [4, 9]. The window material was 0.006mm Kapton[®] (Dupont H-film), with gold vacuum-deposited on both sides (40-50 Å on the outer surface, 120-150 Å on the inner surface). A bias voltage of 2150 V was applied to the detector, which was the voltage closest to the center of the beta counting plateau [4].

Gas proportional detectors utilize gas multiplication, where free electrons generated by the ionization of the gas by the incoming particles are accelerated by the strong electric field (created by the bias voltage) to sufficient kinetic energy to cause further ionizations. Electrons freed in these ionizations can also be accelerated to cause additional ionizations, as long as their energy is greater than the ionization energy of the neutral gas molecules. This gas multiplication process, or cascade, is known as a Townsend avalanche, which terminates when all free electrons are collected at the anode [11]. With a well designed and maintained detector, the number of secondary ionizations is proportional to the number of initial ionizations, but multiplied by a factor of “many thousands” [11]. Almost all primary ion pairs are formed outside the multiplying region, which is confined to a small volume around the anode, and the electrons from the primary ionizations drift to that region before multiplication takes place, “therefore, each electron undergoes

the same multiplication process regardless of its position of formation, and the multiplication factor will be [the] same for all original ion pairs.” [11] If the charge pulse of all of the electrons collected at the anode per event is larger than the discriminator level setting after amplification, a count is then recorded by the scaler.

The two sources used in the BNL experiment, ^{32}Si and ^{36}Cl , are described in detail in Alburger, et al., Sec. 2 of Ref. [4]. The isotope ^{32}Si undergoes β^- -decay (100%, $E_{\beta_{max}} = 224.31\text{keV}$) to ^{32}P with a $T_{1/2}=157(19)$ y [23]. The radioactive daughter, ^{32}P , (which is in secular equilibrium with ^{32}Si) undergoes β^- -decay (100%, $E_{\beta_{max}}=1710.5(21)$ keV) to ^{32}S (stable) with a $T_{1/2}=14.262(14)$ d [24]. The isotope ^{36}Cl , on the other hand, decays via competing β -decay branches (β^- , 98.1(1)%, $E_{\beta_{max}}=708.6(3)$ keV; β^+/ϵ , 1.9(1)%) [25]. Great care was taken by the BNL group in preparation of the ^{32}Si source to ensure that no contaminants would be included that would confuse the data collection and analysis. Analyses of the spectra of each of the sources were conducted with a plastic scintillator to test for impurities or other problems, and the spectra were as expected. The ^{32}Si betas were not noticeably evident in the spectrum from the plastic scintillator, which was likely due to the effective thickness of the sample (17 mg/cm^3) that served to degrade and smear the low-energy betas, as noted by Alburger, et al. [4]. However, they did appear with the expected equal distributions when part of the same material was measured in a liquid scintillator [4, 26]. The ^{36}Cl spectrum was as expected, as reported by Alburger, et al. [4].

The gas proportional detector described above was utilized in a differential counter system described in detail in Ref. [9], which used a precision sample changing system that would alternate the sources during counting runs. The system was designed and built to allow maximum reproducibility, e.g. by utilizing precision micrometer heads which adjusted the source/detector distance to within $\pm 0.001\text{mm}$ [9]. As stated before, this system was contained within a “pressure-regulated box in order to minimize the differential energy-loss effects that would occur with changes in barometric pressure” [4]. Tests of the sensitivity of the counting system to changes in the box pressure, as well as to detector bias voltage, detector gas flow, and discriminator setting were carried out prior to the series of measurements, and the estimated effects on the ^{32}Si counts and the Si/Cl ratio are detailed in Table 1 of Ref. [4].

Notwithstanding the tests described above, Alburger, et al. identified an unexpected periodic fluctuation in the Si/Cl ratio with a period of approximately 1 year. Having virtually eliminated other systematic variables, or at least having controlled them to the extent possible, Alburger’s BNL group was left with temperature and humidity as possible explanations, which are known to change the density of air (even if the pressure of the box containing the detector system is held constant). Increases in temperature will decrease the density of air, as will increases in relative humidity, although humidity has a much smaller effect than temperature. To summarize, warmer more humid air, i.e. summer air, is less dense than cooler, drier winter air. This is depicted in Fig. 3, which plots the temperature and relative humidity dependence of the density of air, based on equations

developed and recommended by the Comité International des Poids et Mesures (CIPM) [27, 28, 29].

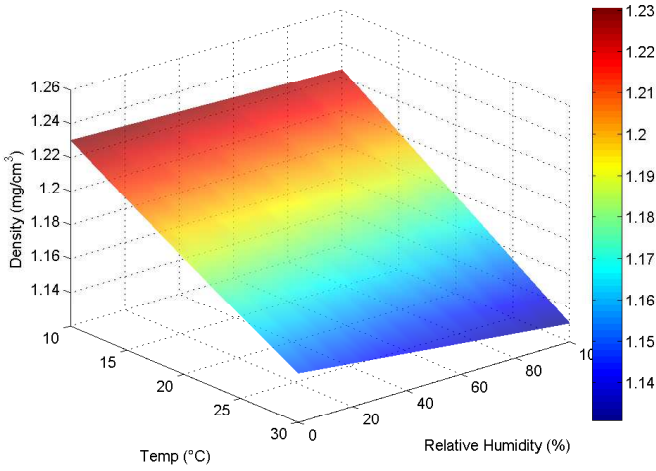


Figure 3: Plot of air density as a function of temperature and relative humidity. The data were calculated based on the formulae presented in Refs. [27, 28, 29]

The Alburger group at BNL did not begin collecting data on temperature and humidity until the last five months of the four year experiment, and during that time saw a range of temperatures of 72.4-74.7°F, and a relative humidity range of 35-76% [4]. However, further investigations into data collected in other laboratories within the same building suggested that the average temperatures remained well within the range of 70-76°F year round. The BNL group noted that the fluctuations appear to follow the same annual cycle as outdoor temperature. They also noted that if the indoor temperature and relative humidity were to track the outdoor conditions, then the data appeared to indicate that the fluctuations were environmentally based. The cooler, drier, and denser winter air could attenuate the lower energy ^{36}Cl betas, and would thus affect the ratio Si/Cl because the lower energy ^{36}Cl counts would be more weather dependent. However, Alburger, et al. concluded that “in order to produce the variations of ± 3 standard deviations, the large humidity changes would have to be combined with temperature variations over a range of at least $\pm 5^\circ\text{F}$, which is larger than the probable actual range. We therefore conclude that systematic periodic variations are present but that they cannot be fully accounted for by our tests or estimates”[4].

The conclusions of the BNL group can be supported by estimating the effect of temperature and relative humidity on the range of betas over the spectrum of energies that would be seen from both sources. The range of an electron can be estimated by utilizing an analysis by Katz and Penfold [30], which provided a range-energy ($R - E_o$) relationship given by:

$$R(\text{mg}/\text{cm}^3) = 412E_o^{1.256-0.0954\ln E_o} \quad (3)$$

The linear range can be derived by dividing R by the density of the propagating medium, air, and expressing the electron energy, E_o in MeV (it should be noted that these linear ranges are not necessarily straight line paths). We utilize the variations

suggested by Alburger, et al. for temperature (T) ($73\pm 5^\circ\text{F}$) and relative humidity (RH) (35-76%), and assume that the maximum density would be associated with the minimum T and RH (68°F , RH=35%), and the minimum air density with the maximum T and RH (78°F , RH=76%). The air densities are then found to be $1.185\text{mg}/\text{cm}^3$ and $1.155\text{mg}/\text{cm}^3$, respectively. The energy-dependent linear ranges of energetic electrons for each condition set are shown in Fig. 4, which gives the linear range of betas of various low energies in air. We have neglected the effects of the energy losses due to transport through the detector window or sources, which are assumed to be independent of temperature. It should be noted again, that the ^{36}Cl source was 4mm from the detector window, and the ^{32}Si source 1mm away. Fig. 4 confirms the conclusions of the BNL group that changes in T and/or RH would have been too small to explain the fluctuations in their data. These conclusions are further supported by an MCNP analysis which we have carried out, the results of which will be described below. Before turning to this analysis, we first consider the remaining question of backgrounds which could impact the BNL detector system.

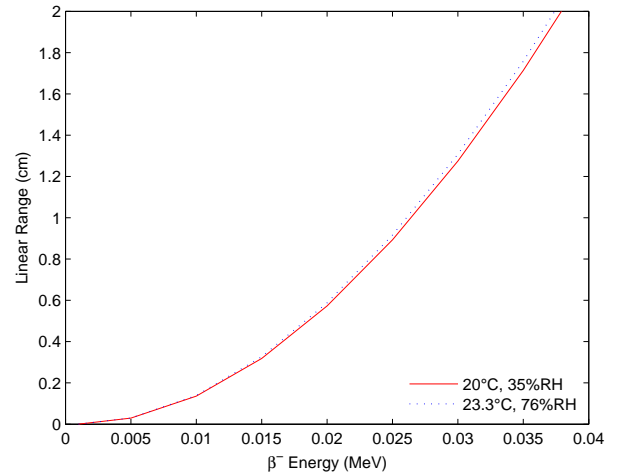


Figure 4: Linear range of betas in air as a function of beta energy. The graphs are calculated using the results of Katz and Penfold in Ref. [30]. The air densities shown are based on the maximum and minimum values of temperature and humidity quoted by Alburger, et al. in Ref. [4]

The BNL group measured an initial background counting rate of 6.6(3)/min. This background measurement was repeated after the conclusion of all runs by counting with the ^{32}Si source removed from its holder, and the ^{36}Cl still in place (to ensure that there was no cross-talk between the sources). The rate was found to be 6.5(3)/min. Since the average count rates for the measurements were initially substantially larger, 21,500/min and 14,800/min for the ^{36}Cl source and ^{32}Si source, respectively, the background count rates were considered insignificant, and hence were ignored by the BNL group. Additionally, since the sources were alternated during the counting procedure for each run, 30 minutes each for 20 cycles, the background would likely be the same for both of the isotopes.

5. Monte Carlo Modeling of the BNL Detector

The Monte Carlo radiation transport software package, MCNPX [31], was used to determine the effects of changes in ambient air temperature on the proportional detector system used by Alburger et al. [4]. The air density between the source and detector window was varied over the temperature range 40°F-90°F by use of the ideal gas law, corresponding to an approximate density range between $1.1350 \times 10^{-3} \text{g/cm}^3$ and $1.2486 \times 10^{-3} \text{g/cm}^3$ for dry air. While humidity also affects total air density, this effect is presumed to be small (see Fig. 3) relative to the effects of temperature change, and hence was ignored in this study. Additionally, the 40-90°F range that was analyzed encompasses both the minimum and maximum air densities expected for a wide range of both temperature and humidity in the laboratory. The physical parameters of the detector system (including the proportional detector, ^{32}Si source, and ^{36}Cl source) were obtained from the literature [4, 9], the BNL group's experimental notes (private communication, D. Alburger and G. Harbottle, 2005), and measurements of both the actual sources used in the experiment and a proportional detector of similar design.

The cylindrical end-window proportional detector was modeled as a stainless steel (type 304) cylindrical shell with inner diameter 3.96875 cm, length 5.08 cm, and 3 mm wall thickness. The detector window was modeled following Harbottle et al. [9] as 0.006 mm Kapton[®] plated with vacuum-deposited gold on both the inner (125 Å) and outer (45 Å) surfaces. The detector volume was filled with P-10 gas (90% argon, 10% methane by volume) with a calculated density of $1.6773 \times 10^{-3} \text{g/cm}^3$. This gas density within the detector was held constant.

Due to the possibility that the lower energy betas from ^{36}Cl (708.6keV) were more easily affected by changes in air density than the higher energy ^{32}Si - ^{32}P betas (1710.5keV), each source was modeled separately, which also allowed us to account for the difference in proximity of each source to the detector. The ^{32}Si source, which was modeled in detail as described by Alburger et al. [4], consisted of a brass base 3.18 cm in diameter and approximately 0.3175 cm (1/8 in.) thick with a 1.91-cm-diameter, 0.8-mm-deep recess. The recess contained 47.7 mg of SiO_2 covered by 9.263×10^{-5} cm of aluminum foil. The MCNPX electron source volume was defined uniformly over the volume occupied by the SiO_2 . According to Alburger et al., the $^{32}\text{SiO}_2$ source was created approximately 13 years prior to the start of the half-life experiment [4], and hence ^{32}Si was certainly in secular equilibrium with its radioactive daughter, ^{32}P , during the experimental time frame. The source energy spectrum used in these MCNPX models consisted of equal contributions from the ^{32}Si ($E_{max} = 225$ keV) and ^{32}P ($E_{max} = 1710.5$ keV) beta energy spectra calculated according to Fermi theory, which allowed us to incorporate the loss of the much lower energy betas from ^{32}Si .

As was the case for the ^{32}Si source, the ^{36}Cl source was placed on a brass base 3.18 cm in diameter and 0.3175 cm thick, but without a recess machined into the top. The ^{36}Cl was spread over a diameter of 1.91 cm in the center of the top surface of the base. Thus, the MCNPX electron source was defined as a flat

disk 1.91-cm in diameter on the surface of the brass base with an energy spectrum equal to that of ^{36}Cl ($E_{max} = 709.2$ keV) calculated according to Fermi theory.

According to the BNL experimental notes, the distance of each source from the detector window was adjusted in order to obtain similar count rates from each, and this was achieved by having the ^{32}Si source 1.000 mm from the detector window, while the ^{36}Cl was placed at a distance of 4.000 mm. The source position in the MCNPX models for each source reflected these distances.

As stated before, Alburger, et al. reported [4] that the temperature variation was well within the range 70-76°F. We found that tally values varied so little over this range that they were statistically constant to within the minimum achievable relative error in MCNPX. Thus, a large temperature range of 40°F to 90°F was chosen to improve the statistical determination of the function relating each tally to air temperature (and associated density). The results presented here were obtained using 1×10^8 (for ^{36}Cl) or 2×10^8 (for ^{32}Si - ^{32}P) source electrons for each density variation, and this provided relative errors of $\sim 10^{-4}$ for the particle/energy current tallies, and $\sim 2 \times 10^{-4}$ for the energy deposition tallies.

A number of MCNPX tallies were used to test the assertion that variations in air density with temperature would result in an associated increase or decrease in the probability that an electron with a given energy will traverse the air gap between the source and detector window. A linear least-squares fit was applied to the results of each tally as a function of air temperature, and these results are summarized in Table 1.

Of particular interest are the temperature dependent variations in the energy deposition within the detector (Fig. 5), the electron current at the detector window (Fig. 6), and the energy current at the detector window (Fig. 7), all of which can be used as surrogates for detector count rate. For each of these tallies, ratios of the value per source electron for ^{32}Si to that of ^{36}Cl were calculated. Energy deposition, electron current, and energy current ratios were found to vary by $1.77(40) \times 10^{-5}/^\circ\text{F}$, $1.46(21) \times 10^{-5}/^\circ\text{F}$, and $3.52(48) \times 10^{-5}/^\circ\text{F}$, respectively. These results are echoed by the tally variations as a function of temperature for ^{32}Si - ^{32}P and ^{36}Cl individually in Table 1. As expected, all individual tally values increase with increasing temperature due to the associated decrease in air density between the source and detector. In all cases, the rate of change is greater for ^{36}Cl due to its lower energy spectrum (relative to ^{32}P) and greater source-detector distance. In general, detector events arising from the ^{32}Si source are due almost entirely to ^{32}P betas because the low-energy ^{32}Si betas are largely attenuated by the source itself [4]. This explains the negative slope associated with the Si/Cl ratios as temperature increases.

The ratios of electron current and energy current across a plane just above the source, and above the detector window were also examined (see Figures 8 and 9). These ratios directly address the assertion that changes in air density result in count rate variations due to increased or decreased absorption of electrons in the air gap between source and detector. The ^{32}Si electron and energy current ratio dependence was found to be $6.8(32) \times 10^{-6}/^\circ\text{F}$ and $5.1(33) \times 10^{-6}/^\circ\text{F}$, respectively, and for

Table 1: Table of MCNPX results showing the sensitivities of the system per degree Fahrenheit.

	^{32}Si - ^{32}P		^{36}Cl		$(^{32}\text{Si}$ - $^{32}\text{P})/^{36}\text{Cl}$ Ratio
	Per Source e^-	Norm.(70°F)	Per Source e^-	Norm.(70°F)	
Det. E Deposition (MeV/ptcl) ($\Delta/^\circ\text{F}$)	$0.051(24) \times 10^{-6}$	$10.1(67) \times 10^{-6}$	$0.34(40) \times 10^{-6}$	$39.8(67) \times 10^{-6}$	$-17.7(40) \times 10^{-6}$
Det. Window e^- Current ($\Delta/^\circ\text{F}$)	$4.39(86) \times 10^{-6}$	$12.1(33) \times 10^{-6}$	$20.3(13) \times 10^{-6}$	$35.3(33) \times 10^{-6}$	$-14.6(21) \times 10^{-6}$
Det. Window E Current (MeV/ptcl) ($\Delta/^\circ\text{F}$)	$1.48(45) \times 10^{-6}$	$7.8(33) \times 10^{-6}$	$4.32(32) \times 10^{-6}$	$32.4(34) \times 10^{-6}$	$-35.2(48) \times 10^{-6}$
Det./Source e^- Current Ratio ($\Delta/^\circ\text{F}$)	$6.8(32) \times 10^{-6}$	$7.1(48) \times 10^{-6}$	$29.5(24) \times 10^{-6}$	$41.5(48) \times 10^{-6}$	$-46.5(64) \times 10^{-6}$
Det./Source E Current Ratio ($\Delta/^\circ\text{F}$)	$5.1(33) \times 10^{-6}$	$5.2(47) \times 10^{-6}$	$24.9(25) \times 10^{-6}$	$33.7(48) \times 10^{-6}$	$-37.9(63) \times 10^{-6}$

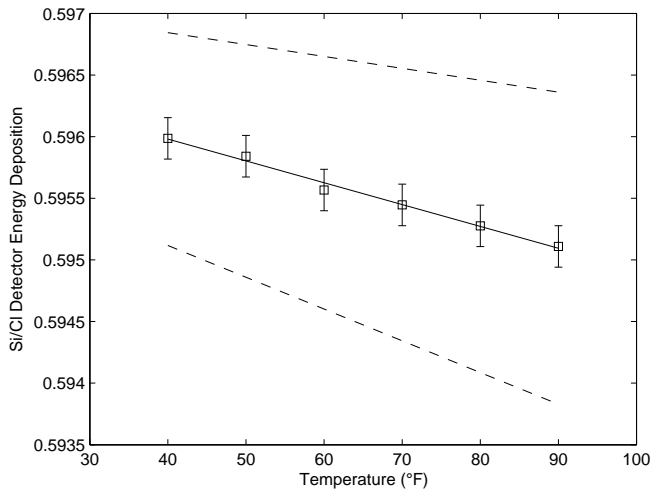


Figure 5: The ratio of ^{32}Si to ^{36}Cl energy deposition in the proportional detector. Dashed lines indicate the 95% confidence interval for the calculated linear least-squares fit of the data.

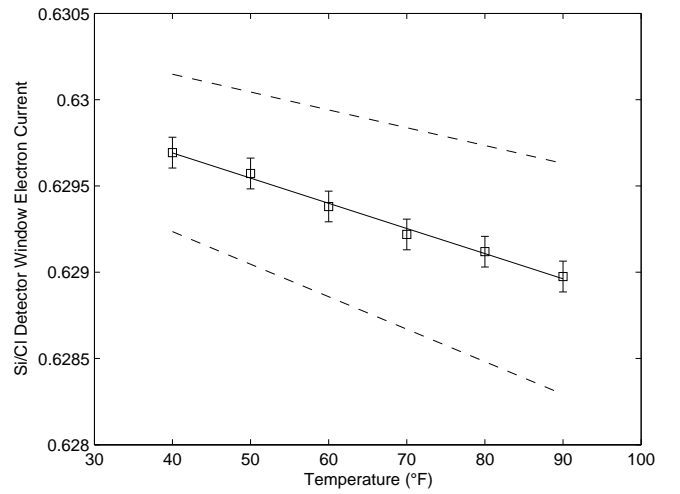


Figure 6: The ratio of ^{32}Si to ^{36}Cl electron current (number of electrons) across the proportional detector window (into the detector). Dashed lines indicate the 95% confidence interval for the calculated linear least-squares fit of the data.

^{36}Cl , $2.95(24) \times 10^{-5}/^\circ\text{F}$ and $2.49(25) \times 10^{-5}/^\circ\text{F}$, respectively. These temperature dependencies are all approximately 2 orders of magnitude smaller than the periodic variations observed by Alburger et al.

As we noted previously, following a number of experimental tests, Alburger et al. concluded that it was possible that part of the 0.3% annual variation in observed count rates could be attributed to changes in ambient temperature (between 70 and 76 °F), and relative humidity (35 to 76%) [4]. However, the results obtained in this Monte Carlo analysis indicate that a temperature variation much larger than 6°F would be required to generate the observed count rate oscillations. Given that the ratio of energy deposition in the detector varies by approximately $1.2 \times 10^{-5}/^\circ\text{F}$, the temperature of the air separating the source from the detector would have had to vary by well over 100 °F to account for the observed data. We therefore conclude that changes in temperature and relative humidity alone could not have caused the observed periodic count rate variations.

6. Further Analysis

In Fig. 10, we exhibit the count rate ratio $\text{Si}/\text{Cl} \equiv \dot{N}(\text{Si})/\dot{N}(\text{Cl})$ as a function of time, along with the outdoor temperature variation for the area surrounding the BNL [32] and $1/R^2$. We see that Si/Cl approximately correlates with $1/R^2$ and anti-correlates with temperature, in both cases with observable phase shifts. Since at this stage we have no theoretical reason to suppose that Si/Cl should correlate (rather than anti-correlate) with $1/R^2$, both of the correlations in Fig. 10 are significant. However, we have already ruled out temperature as the primary explanation of the Si and Cl individual fluctuations, and hence we wish to understand whether influences emanating from the Sun, such as neutrinos, could be compatible with these data.

In such a picture, the effect of analyzing the ratio Si/Cl is to largely cancel out small fluctuations in voltage, currents, temperature, background, etc., which are common to both $\dot{N}(\text{Si})$ and $\dot{N}(\text{Cl})$, while leaving intact the presumably larger effects due to the variation of $1/R^2$. From this perspective, the fact that the Si/Cl ratio does not exactly track $1/R^2$ is understandable in

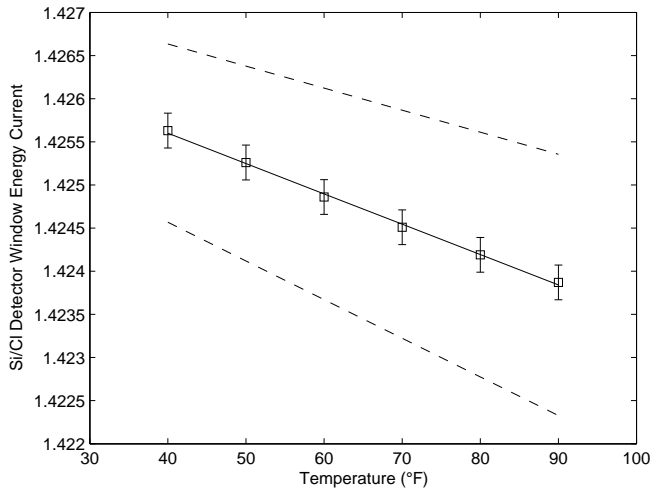


Figure 7: The ratio of ^{32}Si to ^{36}Cl energy current (MeV) across the proportional detector window (into the detector). Dashed lines indicate the 95% confidence interval for the calculated linear least-squares fit of the data.

terms of the differing sensitivities of Si and Cl to external perturbations: the same nuclear structure mechanisms which endow Si and Cl with very different lifetimes (172y and 301,000y, respectively) could presumably result in different responses of these nuclei to small perturbations. Evidence of this effect was first pointed out by Ellis [33], who saw an annual periodic signal in ^{56}Mn , but not in ^{137}Cs when both nuclides were measured for several years on the same detector system. Therefore, a long-term periodic signal due to the variation of $1/R^2$ would survive in the ratio of Si/Cl. This can be understood quantitatively by writing

$$\begin{aligned} \frac{\dot{N}(\text{Si})}{\dot{N}(\text{Cl})} &= \frac{A(\text{Si}) [1 + \epsilon(\text{Si}) \cos \omega t]}{A(\text{Cl}) [1 + \epsilon(\text{Cl}) \cos \omega t]} \\ &\cong \frac{A(\text{Si})}{A(\text{Cl})} \{1 + [\epsilon(\text{Si}) - \epsilon(\text{Cl})] \cos \omega t\}. \end{aligned} \quad (4)$$

Here A, B, and ϵ are constants, with $\epsilon(\text{Si}) \neq \epsilon(\text{Cl})$, and $\epsilon \ll 1$ has been assumed. In summary, Fig. 10 is compatible with a picture in which any differences between Si/Cl and $1/R^2$ are due to the varying sensitivities of Si and Cl to an external perturbation coming from the Sun, as seen in Ellis' data. Although a differential temperature effect could in principle also explain Fig. 10, this would require temperature-dependent effects which are much larger than allowed by the preceding analysis.

7. Gravitational and Related Influences

The preceding discussion leads naturally to the question of whether the observed effects in the BNL and PTB data could arise from a change in the gravitational potential of the Sun at the respective detectors as the Earth passes from perihelion to aphelion and back. In the framework of conventional General Relativity (GR) all clocks at a given space-time point run at the same rate, irrespective of their internal mechanism. In terms of Eq. 4 this would correspond to setting $\epsilon(\text{Si}) = \epsilon(\text{Cl})$, in which

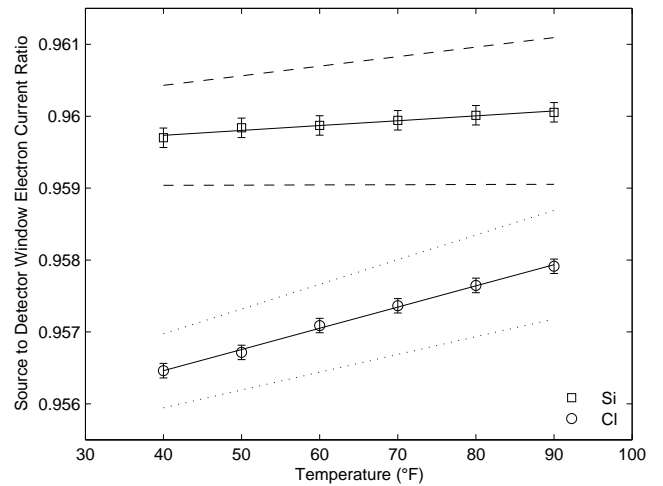


Figure 8: The ratios of electron current exiting the source toward the detector and electron current across the proportional detector window (into the detector) for ^{32}Si and ^{36}Cl . ^{36}Cl data have been shifted up by 0.2465 to facilitate visualization of both curves. Dashed and dotted lines indicate the 95% confidence interval for the calculated linear least-squares fit of the data for ^{32}Si and ^{36}Cl , respectively.

case there would be no fluctuation in the ratio Si/Cl. Since this is in obvious disagreement with the BNL data, conventional GR can be ruled out as an explanation of the observed effects.

However, this conclusion does not necessarily hold for various alternatives to GR. Will [34] has shown that in non-metric theories, clocks of different construction can in fact behave differently in a gravitational field. Although such a mechanism is possible in principle, it fails in practice on quantitative grounds. The Sun's gravitational potential $\Phi = GM_{\odot}/Rc^2$ at the Earth is $\Phi = 9 \times 10^{-9}$, and the fractional change $\Delta\Phi$ between perihelion and aphelion is $\Delta\Phi = 3 \times 10^{-10}$. An effect this small would be undetectable given the BNL and PTB statistics, even if the coefficients multiplying $\Delta\Phi$ in a non-metric theory were relatively large. Additionally, constraints on parameters which measure deviations from GR are sufficiently restrictive [35] to preclude the possibility of explaining the BNL and PTB data in terms of any known alternative to GR.

A class of gravity-related theories which cannot be excluded at present are those in which scalar fields are introduced to induce a time variation in fundamental constants such as the fine structure constant $\alpha = e^2/\hbar c$. We have discussed elsewhere [3] the possibility that although the simplest such theories cannot account for the BNL or PTB data, theories in which two or more scalar fields are introduced which influence both α and the electron/proton mass ratio (and possibly other quantities) might work.

8. Environmental Influences During the Solar Flare of 2006 December 13

We turn in this section to a discussion of possible environmental influences on the NaI detector system used in [1] during

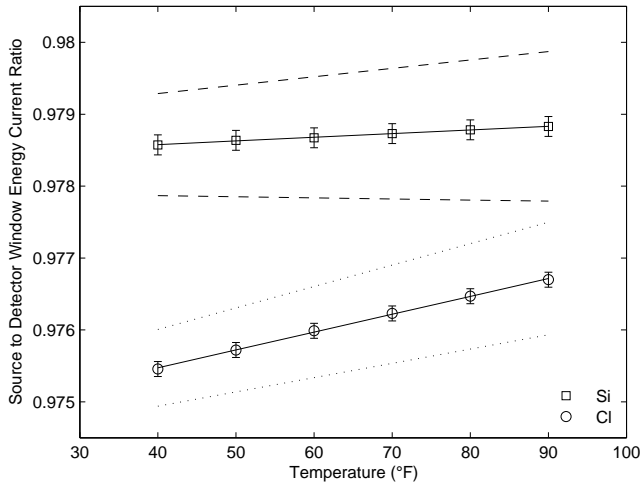
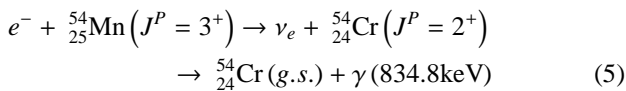


Figure 9: The ratios of energy current exiting the source toward the detector and energy current across the proportional detector window (into the detector) for ^{32}Si and ^{36}Cl . The ^{36}Cl data have been shifted up by 0.2390 to facilitate visualization of both curves. Dashed and dotted lines indicate the 95% confidence interval for the calculated linear least-squares fit of the data for ^{32}Si and ^{36}Cl , respectively.

the 2006 December 13 solar flare. This is motivated by the potential connections between the ^{54}Mn decay data collected in the time period surrounding the flare, and the BNL and PTB decay data which are the primary focus of the present paper. As we have already noted in the Introduction, the short duration of the solar flare allows us to rule out seasonal temperature, humidity and pressure influences on the detector system as potential explanations of the observed decrease in the ^{54}Mn counting rate. Hence the focus of this section will be on other possible “environmental” influences on the detector system during the solar flare, such as neutrons, muons, etc.

Although cosmic ray particles are known to be capable of influencing some detectors, there is a generic argument against any mechanism which attributes the drop in the ^{54}Mn count rate to cosmic rays. This is based on the observation that the signal for a ^{54}Mn decay in our system is the detection of the characteristic 834.8 keV photon resulting from the electron-capture process,



Hence the 834.8 keV photon which signals the electron-capture process is uniquely associated with the specific transition of the excited $^{54}_{24}\text{Cr}$ from the excited $J^P = 2^+$ state to the $J^P = 0^+$ ground state (g.s.). The data points utilized in Ref. [1] represent the integral count within the Region of Interest (ROI) set on the 834.8 keV photon for a four hour live-time. Even if there had been a large change in the cosmic ray flux of neutrons or muons during the flare, the chance that the nuclear or electromagnetic interactions induced by these particles would have accidentally

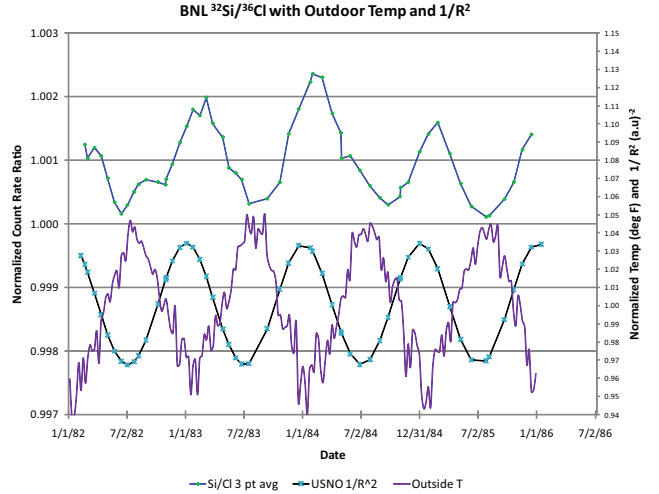


Figure 10: The counting rate ratio $\tilde{N}(\text{Si})/\tilde{N}(\text{Cl})$ for the BNL data as a function of time, along with $1/R^2$ and the outdoor temperature measured by NOAA near BNL. The correlation with $1/R^2$ and the anti-correlation with temperature are both evident. See text for further discussion.

produced a photon at 834.8 keV, or deposited the energy equivalent of 834.8 keV within the NaI crystal, is extremely small. Moreover, the fact that a deficit of counts appeared in the ROI, and not an increase, indicates that this already very remote possibility is highly unlikely. It is also unlikely that counts were selectively removed from the ROI as a result of changes to the cosmic ray flux. An alternative explanation might be that an increase in the cosmic ray flux would generate a large distribution of energy depositions across the energy spectrum, and thus change the system dead time, leading to a loss of counts within the ROI. Dead time was tracked as a variable, however, and did not show changes over the course of the flare when compared to the counts preceding or following the flare period. Additionally, inspection of the spectra files also show no significant changes in the counts of channels above or below the 834.8 keV ^{54}Mn peak.

The above argument is bolstered by observations made by other groups during the 2006 December 13 flare. Although an analysis of data from world-wide neutron monitors by Bütikofer, et al. and Plainaki, et al. [36, 37] exhibited a $\sim 90\%$ increase in the 1-minute data at Oulu and Apatity, the overall neutron flux was still so small as to have a negligible effect on the detector system. This is particularly true in light of the fact that the NaI detector is insensitive to neutrons, and the flux of neutrons was too low to affect the ^{54}Mn sample directly.

Similar arguments allow us to exclude a change in the flux of cosmic ray muons resulting from a Forbush decrease [38] as a possible explanation of the flare data. A Forbush decrease is a rapid change in the flux of cosmic rays resulting from plasma clouds emitted by the Sun during a solar storm [38]. Evidence for a Forbush decrease during the 2006 December 13 flare obtained from the muon telescopes at the Basic Environmental Observatory (BEO) in Bulgaria and from Nagoya, Japan are shown in Figs. 5 and 6 of Ref. [38], respectively. The BEO data exhibited a sharp Forbush decrease beginning at $\sim 15:30-16:30$

UT on 2006 December 14, and reached a maximum at 05:00 UT on December 15. The beginning of the Forbush decrease thus occurred 37 hours *after* the dip in the ^{54}Mn counting rate reported in Ref. [1], which coincided in time with the solar flare at $\sim 02:40$ UT on December 13. Additionally, the minimum in the muon count rate associated with the Forbush decrease was observed more than 2 days later. The data from the BEO are supported by data obtained at Nagoya, which exhibited a similar time-dependence [38]. Given the timing of the Forbush decrease relative to the dip in the ^{54}Mn counting rate we can thus reasonably conclude that the dip was not likely the result of the response of the detector system to the Forbush decrease.

The preceding arguments can be further strengthened by noting from Ref. [1] that the ^{54}Mn count rate started to decrease ~ 1.7 days *before* the flare. It follows that the beginning of the decrease in the ^{54}Mn count rate preceded the beginning of the Forbush decrease by more than 70 hours, and hence was not caused by it.

In summary, we can rule out environmental explanations of the correlation between the solar flare of 2006 December 13 and the observed dip in our ^{54}Mn data [1] on several grounds. These include, (a) the observation that the solar flare lasted approximately 43 minutes, which is too short a time for seasonal environmental influence to have affected the detector system. (b) the failure of these mechanisms to produce the characteristic 834.8 keV photon arising from ^{54}Mn electron capture, or to account for the ~ 1.7 day precursor signal observed in the ^{54}Mn decay data; (c) the timing of the Forbush decrease which followed, rather than preceded, the dip in the ^{54}Mn data. Additionally, the observed changes in cosmic ray fluxes would have been too small quantitatively to account for the ^{54}Mn data.

9. Discussion and Conclusions

As we noted in the Introduction, there are at present two competing general explanations for the apparent fluctuations observed in the BNL and PTB data: (a) they arise from the responses of the respective detector systems to seasonal variations in temperature, pressure and humidity, and possibly other factors such as radon buildup. (b) the fluctuations arise from the decay process itself, due to some as yet unknown influence possibly originating from the Sun. By modeling the respective detector systems in detail, we have shown here that alternative (a) is an unlikely explanation for the observed BNL and PTB data, and hence by implication alternative (b) is more likely to be correct. The resulting inference, that nuclear decay rates are being directly influenced by solar activity is further supported by our analysis of ^{54}Mn decay data acquired during the solar flare of 2006 December 13, which we have also analyzed. Our conclusion that the dip in the ^{54}Mn data, which was coincident in time with the flare, was not likely attributable to changes in the cosmic ray flux during the flare, further strengthens the case that nuclear decays are being directly affected by solar activity. This inference can evidently be checked in a variety of experiments such as those described on Ref. [3], some of which are already in progress.

10. Acknowledgments

The authors wish to thank D. Alburger and G. Harbottle for making their raw BNL data, apparatus, and samples available to us, and for many helpful conversations. We are also deeply grateful to H. Schrader for the raw PTB decay data, as well as for invaluable discussions on his experiment during our visit to the PTB. We are indebted to our colleagues who have helped us in this work, including V. Barnes, J. Buncher, T. Downar, D. Elmore, A. Fentiman, J. Heim, M. Jones, A. Karam, D. Krause, A. Longman, J. Mattes, E. Merritt, H. Miser, T. Mohsinally, S. Revankar, B. Revis, A. Treacher, J. Schweitzer, and F. Wissman. The work of EF was supported in part by the U.S. Department of Energy under Contract No. DE-AC02-76ER071428.

References

- [1] J. H. Jenkins, E. Fischbach, Perturbation of nuclear decay rates during the solar flare of 2006 December 13, *Astropart. Phys.* 31 (6) (2009) 407–411.
- [2] J. H. Jenkins, E. Fischbach, J. B. Buncher, J. J. Mattes, D. E. Krause, J. T. Gruenwald, Evidence of correlations between nuclear decay rates and Earth-Sun distance, *Astropart. Phys.* 32 (1) (2009) 42–46.
- [3] E. Fischbach, J. Buncher, J. Gruenwald, J. Jenkins, D. Krause, J. Mattes, J. Newport, Time-dependent nuclear decay parameters: New evidence for new forces?, *Space Sci. Rev.* 145 (3) (2009) 285–335.
- [4] D. E. Alburger, G. Harbottle, E. F. Norton, Half-life of ^{32}Si , *Earth and Planet. Sci. Lett.* 78 (2-3) (1986) 168–76.
- [5] H. Siebert, H. Schrader, U. Schoetzig, Half-life measurements of europium radionuclides and the long-term stability of detectors, *Appl. Rad. and Isot.* 49 (9-11) (1998) 1397–1401.
- [6] H. Schrader, Transmission of ^{226}Ra data.
- [7] O. P. Verkhoglyadova, L. Gang, G. P. Zank, H. Qiang, Modeling a mixed SEP event with the PATH model: December 13, 2006 1039 (2008) 214–219.
- [8] T. M. Semkow, D. K. Haines, S. E. Beach, B. J. Kilpatrick, A. J. Khan, K. O'Brien, Oscillations in radioactive exponential decay, *Phys. Lett. B* 675 (5) (2009) 415–419.
- [9] G. Harbottle, C. Koehler, R. Withnell, A differential counter for the determination of small differences in decay rates, *Rev. of Sci. Instrum.* 44 (1) (1973) 55–9.
- [10] H. Schrader, Ionization chambers, *Metrologia* 44 (4) (2007) 53–66.
- [11] G. F. Knoll, Radiation detection and measurement, 3rd Edition, John Wiley & Sons, New York, 2000.
- [12] C. G. Found, Ionization potentials of argon, nitrogen, carbon monoxide, helium, hydrogen and mercury and iodine vapors, *Phys. Rev.* 16 (1) (1920) 41.
- [13] S. Okabe, T. Nishikawa, M. Aoki, M. Yamada, Looping variation observed in environmental gamma-ray measurement due to atmospheric radon daughters A255 (1987) 371–3.
- [14] T. Nishikawa, S. Okabe, M. Aoki, Seasonal variation of radon daughter concentrations in the atmosphere and in precipitation at the Japanese coast of the sea of Japan 24 (1988) 93–5.
- [15] J. C. H. Miles, R. A. Algar, Variations in radon-222 concentrations, *Jour. of Radiologic. Prot.* 8 (2) (1988) 103–105.
- [16] M. I. Gaso, M. L. Cervantes, N. Segovia, V. H. Espindola, Atmospheric radon concentration levels, *Radiat. Meas.* 23 (1) (1994) 225–30.
- [17] M. C. Thorne, Background radiation: natural and man-made, *Jour. of Radiologic. Prot.* 23 (1) (2003) 29–42.
- [18] A. Abbady, A. G. E. Abbady, R. Michel, Indoor radon measurement with the lucas cell technique, *Appl. Rad. and Isot.* 61 (6) (2004) 1469–1475.
- [19] F. Wissmann, Variations observed in environmental radiation at ground level, *Radiat. Protect. Dosimetry* 118 (1) (2006) 3–10, 10.1093/rpd/nci317.
- [20] T. Szegvary, F. Conen, P. Ciais, European ^{222}Rn inventory for applied atmospheric studies, *Atmospheric Environment* 43 (8) (2009) 1536–1539.
- [21] H. Schrader, Calibration and consistency of results of an ionization-chamber secondary standard measuring system for activity, *Appl. Rad. Isot.* 52 (3) (2000) 325–334.

- [22] A. Artna-Cohen96, Nuclear data sheets for Eu-152, Nucl. Data Sheets 79 (1).
- [23] B. Singh, Nuclear data sheets for ^{32}Si , Tech. rep. (2006).
- [24] P. M. Endt, R. B. Firestone, Nuclear data sheets for ^{32}P , Tech. rep. (1999).
- [25] P. M. Endt, R. B. Firestone, Nuclear data sheets for ^{36}Cl , Tech. rep. (1999).
- [26] J. B. Cumming, Assay of silicon-32 by liquid scintillation counting, Radiochem. and Radioanalyt. Lett. 58 (5-6) (1983) 297–305.
- [27] P. Giacomo, Equation for the determination of the density of moist air (1981), Metrologia 18 (3) (1982) 171–171.
- [28] R. S. Davis, Equation for the determination of the density of moist air (1981/91), Metrologia 29 (1) (1992) 67–70.
- [29] A. Picard, R. S. Davis, M. Glaser, K. Fujii, Revised formula for the density of moist air (CIPM-2007), Metrologia 45 (2) (2008) 149–155.
- [30] L. Katz, A. S. Penfold, Range-energy relations for electrons and the determination of beta-ray end-point energies by absorption, Rev. Mod. Phys. 24 (1952) 28–44.
- [31] Los Alamos National Laboratory, MCNPX User's Manual, Version 2.6.0, la-cp-07-1473 Edition (April 2008).
- [32] NCDC, National climatic data center: Land-based data (June 2009). URL <http://www.ncdc.noaa.gov/oa/land.html>
- [33] K. J. Ellis, The effective half-life of a broad beam $^{238}\text{Pu}/\text{Be}$ total body neutron irradiator, Phys. Med. Biol. 35 (8) (1990) 1079.
- [34] C. M. Will, Gravitational red-shift measurements as tests of non-metric theories of gravity, Phys. Rev. D 10 (8) (1974) 2330.
- [35] C. M. Will, Theory and experiment in gravitational physics, rev. Edition, Cambridge University Press, Cambridge [England] ; New York, NY, USA, 1993.
- [36] R. Bütikofer, E. O. Flückiger, L. Desorgher, M. R. Moser, B. Pirard, The solar cosmic ray ground-level enhancements on 20 January 2005 and 13 December 2006, Adv. Space Res. 43 (4) (2009) 499.
- [37] C. Plainaki, H. Mavromichalaki, A. Belov, E. Eroshenko, V. Yanke, Modeling the solar cosmic ray event of 13 December 2006 using ground level neutron monitor data, Adv. in Space Res. 43 (4) (2009) 474.
- [38] I. Angelov, E. Malamova, J. Stamenov, The Forbush decrease after the GLE on 13 December 2006 detected by the muon telescope at BEO - Moussala, Adv. Space Res. 43 (4) (2009) 504.